Evidence for a Binary origin of the Young Planetary Nebula HB 12

Chih Hao Hsia[1,2],Wing Huen Ip[1],Jin Zeng Li[2]

[1]*Institute of Astronomy, National Central University, Chung Li 32054, Taiwan (E-mail: d929001@astro.ncu.edu.tw)*

[2]*National Astronomical Observatories, Chinese Academy of Sciences, Beijing 100012, China (E-mail: ljz@bao.ac.cn)*

ABSTRACT

Young planetary nebulae play an important role in stellar evolution when intermediate- to low-mass stars ($0.8 \sim 8$ $M_\odot$) evolve from the proto-planetary nebulae phase to the planetary nebulae phase. Many young planetary nebulae display distinct bipolar structures as they evolve away from the proto-planetary nebulae phase. One possible cause of their bipolarity could be due to a binary origin of its energy source. Here we report our detailed investigation of the young planetary nebula, Hubble 12, which is well-known for its extended hourglass-like envelope. We present evidence with time-series photometric observations the existence of an eclipsing binary at the center of Hubble 12. Low-resolution spectra of the central source show, on the other hand, absorption features such as CN, G-band & Mg b$''$, which can be suggestive of a low-mass nature of the secondary component.

Subject headings: Hubble 12,bipolar structure: general — planetary nebula: individual (Hubble 12) — stars:binary systems

1. Introduction

The young planetary nebula (PN) Hubble 12 (HB 12; PN G111.8-02.8) plays an important role in the study of PNe. The line ratios of its strong fluorescent molecular hydrogen emission (Dinerstein et al., 1988) match closely pure fluorescent emission (Black and van Dishoeck, 1987), which might have originated from shock excitation via collisional interaction of a strong wind from the central star against a circumstellar gaseous disk (Kastner et al., 1994). Particular interest also comes from its bipolar structure of HB 12. Early radio continuum observations from VLA (Bignell, 1983) first disclosed its bipolar configuration.

Miranda and Solf (1989) later confirmed the double lobe structure along the north-south axis through long-slit spectroscopy. In addition, Hora & Latter (1996) and Welch et al. (1999) showed the existence of a ring-like structure near the central core from near-infrared and [Fe II] imaging. Recent HST/NICMOS observations have revealed clearly detailed structure of the inner torus and its bipolar lobes (Hora et al., 2000). The origin of the axis-symmetric morphology of young PNe has long been an unresolved issue. In classification of PNe based on their morphology, Zuckerman and Aller (1986) and Soker (1997) found that a large majority of PNe have non-spherical shapes, some indicate extreme bipolar or axis-symmetric appearance. Such structures could be generated by strong bipolar outflows during the late AGB or post-AGB phase and may be a transient phenomineon (Kwok et al., 2000). The bipolar flows in turn could be produced by close binaries (Morris, 1990; Soker et al., 1998; Soker, 2000) or rather focusing effects from the associated magnetic field (Garcia-Segura et al., 1999, 2000) among various potential mechanisms suggested. Note that observational evidence has been found in support of the binary model (De Marco et al., 2004; Hillwig, 2004; Sorensen and Pollacco, 2004). Detailed investigations of the physical nature and dynamical properties of the central source is therefore of fundamental importance to our understanding of the origin and evolution of PNe.

We have initiated a program combining efforts from the photometric measurements obtained by the one-meter telescope (LOT) on the Lulin Observatory at central Taiwan and the spectrographic observations carried out with the 2.16 m telescope at the Xing-Long station of the National Astronomical Observatory of the Chinese Academy of Sciences (NAOC). Our main objective is to search for the possible presence of periodic variations in the lightcurves of the nucleus of HB 12, NSV 26083. Properties of the binary components could also be inferred from perhaps spectral observations of the central source. We describe, in Section 2, the observations and data reduction. The photometric lightcurves are presented in Section 3, and then a discussion of the results and interpretations in Section 4. The spectral features possibly originating from the cool secondary are investigated in Section 5, which is followed by a summary of the main results of this study.

2. Observations and Data Reduction

2.1. Time-series Broadband Photometric Imaging

High-speed broadband photometric observations were performed in the queue mode on the nights of December 3-5, 2003 using Johnson R and I band filters with the LOT telescope of the National Central University at Taiwan. The camera was operated with a Princeton Instruments 1340 $\times$ 1300 pixel CCD, giving a field of view of $11' \times 11'$. The CCD has a

readout noise of 15.7e and a gain of 4.4. The setup results in a pixel scale of $0.62''$ pixel^{-1}. Flat field exposures were obtained on the twilight sky. The seeing condition all through this run of observations varied between $1.3''$ and $1.9''$. The journal of observations is summarized in Table 1.

More than 800 snap shots of HB 12 were made, with each snap shot containing a 10s exposure in R and another 5s in I. The data reduction includes bias and dark current correction and flat-fielding based on standard packages and procedures in the NOAO IRAF (V2.12). Differential magnitudes of the central core of HB 12 were measured using the DAOPHOT package with three stars in the same field as reference stars. The S/N ratios of all stars are > 100. No apparent variations were found with the reference stars. The differential magnitudes in the R & I bands have an accuracy within 0.04 mag and 0.02 mag, respectively.

2.2. Optical Spectroscopy

Low-resolution spectroscopy was obtained by the 2.16 m telescope of NAOC. The journal of observations in two separate sessions is given in Table 2. In the 2004 session, measurement was performed in the spectral range (4800 - 10500 Å) on the night of Aug. 8, 2004. The spectral dispersion was 3.1 Å pixel^{-1}. A Beijing Faint Object Spectrograph and Camera (BFOSC) and a thinned back-illuminated Orbit 2048 $\times$ 2048 CCD were used. A slit width of $3.6''$ was set. The exposure times ranged from 300 to 900 s. S/N ratios of the continuum of > 90 were achieved. Exposures of Fe-Ne arcs were obtained right before and after each stellar spectrum and used for the wavelength calibration.

In the 2005 session, spectroscopy was performed in the blue (3800 - 6200Å) spectral range on the night of Sep. 26, 2005. The 100 Å mm^{-1} grating was used, which result in a two-pixel resolution of $\sim$ 4.8 Å. The slit was placed at P.A. = 170°, in parallel to the main axis of HB 12 as indicated in Figure 1. The slit width was set to $2''$. An Optomechanics Research Inc. spectrograph and a Tektronix 1024 $\times$ 1024 CCD were used. The exposures ranged from 3600 to 7200 s, resulting in S/N ratios of > 60. Wavelength calibration was performed based on He-Ar lamps exposed right before and after the target spectrum.

The spectral data were reduced following standard procedures in the NOAO IRAF (V2.12) software package. The CCD reductions included bias and flat-field correction, successful background subtraction and cosmic-ray removal. Flux calibration was derived with observations of at least two of the KPNO standard stars per spectral range per night. The atmospheric extinction was corrected by the mean extinction coefficients measured for Xing-

Long station, where the 2.16 m telescope is located.

3. Search for periodicities in the lightcurves

The multi-band photometric results of HB 12 were presented in Figure 2. The method of phase dispersion minimization (PDM, Stellingwerf, 1978) was used to analyze the lightcurves of NSV 26083. The PDM code was employed to derive the period, maximum magnitude and amplitude of the light variation. Before calculating the power spectra, we set the nightly mean magnitude to zero and calculated the amplitude spectra of these data. The I band data clearly covers three primary minima. A linear least square fit results in a period of P = 0.1415 ± 0.0015 days. The R band lightcurve was fitted simultaneously using the period of the I band data because of its distinct existence of primary minima. The power spectra of the photometric data were presented in Figure 3. A prominent amplitude peak is found at 7.06 c/d, which is 3.4 hrs. The corresponding phase diagrams are shown in Figure 4. The profiles are sinusoidal for both the R and I bands. The period shows an amplitude of 0.06 ± 0.0074 mag in R and 0.08 ± 0.0046 mag in I. This suggests that NSV 26083 displays in its multi-band time-series observations periodic variation and indicates probably an eclipsing binary origin of HB 12. It is the first time that a clear signature of periodicity is evidenced toward the exciting source of HB 12, which may have important implications on the physical nature of bipolar structures associated with other young PNe.

Note that the dip in the R band lightcurve seems to be shallower and smoother than that in the I band lightcurve. This wavelength dependence could probably be due to effects from Hα emission of the companion star, which is encompassed by the R band observations, or otherwise reflection effects from the illuminated surface of the less luminous star (Grauer & Bond, 1983; Bruch et al, 2001).

If we alternatively suppose the periodic variations of NSV 26083 are due to rotation modulation of stellar spot(s), the rotational period can be estimated as follows (Reid et al., 1993):

$$P_{crit} = \frac{2\pi R_e^{3/2}}{\sqrt{GM}} = 2.78 R_e^{3/2} M^{-1/2} \tag{1}$$

where P_{crit} is the rotational period of the star in unit of hrs. R_e is the equatorial radius and M the mass of the star in solar units. Following the discussion by Reid et al. (1993), we use R_e = 1.5 R_*, where R_* is the radius of NSV 26083. If Zhang and Kwok's (1993) result for T_{eff} = 31800 K, log g = 3.1 and M = 0.8 $M_\odot$ are adopted, the rotational period P_{crit}

would be as large as 48 hrs. This is inconsistent with our estimation of 3.4 hrs as presented above and helps to exclude the possibility of the modulation by stellar spots.

4. Stellar properties of the binary components

The mass of the central source of HB 12 has been determined to be 0.8 $M_\odot$ by Zhang and Kwok (1993) based on existing infrared and radio data. We present below an estimation of the mass and radius of the proposed secondary component of the system.

First, the secondary star with an orbital period of hours to days was suggested to have a mass of less than 0.5 $M_\odot$ (Chen et al., 1995). If a mass ratio M_2 / M_1 < 0.8 (M_1 is the mass of the primary star) is supposed, the upper limits of the mass and radius of the secondary would satisfy the following condition (Paczyński, 1981):

$$8.85\sqrt{\frac{R_2^3}{M_2}} < P \tag{2}$$

where P is the orbital period in hrs. M_2 and R_2 are the mass and radius of the secondary in solar units, respectively.

Second, assume that the mass-radius relation of the lower main sequence stars can be applied to the secondary (Rappaport et al, 1982):

$$\frac{R_2}{R_\odot} = 0.76(\frac{M_2}{M_\odot})^{0.78} \tag{3}$$

We can combine Eq. (2) with Eq. (3) to obtain

$$M_2 < 0.443 M_\odot \ and \ R_2 < 0.403 R_\odot \tag{4}$$

There is a general agreement (Schönberner, 1981; Heap & Augensen, 1987; Weidemann, 1989; Tylenda et al., 1991b; Zhang & Kwok, 1993; Stasińska et al., 1997) that the dispersion of the central stellar masses of planetary nebulae, averaged to around 0.6 $M_\odot$, should be rather small. If we assume a mass 0.6 $M_\odot$ of the primary star, for M_1 = 0.6 and 0.08 < M_2 < 0.443 , the separation of the stars a = 1.163 ± 0.063 $R_\odot$. In turn, the radius of the Roche lobe of the secondary is ℓ_2 = a [0.5 + 0.227 log (M_2 / M_1)]. This results in an estimation of 0.547 ± 0.03 $R_\odot$ and the hemisphere of the secondary must be illuminated and heated by the primary source.

The distance to HB 12 has been estimated to be 2.24 kpc by Cahn et al. (1992) based on existing optical and radio data, Hora and Latter (1996) determined a E($B-V$) value is 0.28 measuring from the Brackett line flux of the near-IR spectrum, the V magnitude determined by Tylenda et al. (1991a) for the cool stellar component of HB 12 is 13.6. If these results are adopted, the absolute visual magnitude M_v of the central star of HB 12 will be 0.98. Suppose that the primary component has a mass of 0.6 $M_\odot$ and $M_v = 0.98$ at an effective temperature of 31800 K (Zhang and kwok, 1993), the corresponding radius of the primary is estimated to be $R_1 = 0.19\ R_\odot$.

5. The Spectra of NSV 26083

In order to examine the nature of the putative binary companion of NSV 26083, we have initiated a project of spectrographic measurements at the National Astronomical Observatory of the Chinese Academy of Sciences using the 2.16 m telescope. Figure 5 shows the low-resolution spectrum of NSV 26083 taken on August 8, 2004, which apparently indicates various emission lines characteristic of photoionized medium. The profiles of Hα and Hβ are broader than other emission lines, which is here attributed to most likely effects of the Rayleigh-Raman scatting (Arrieta & Torres-Peimbert, 2003).

To search for further evidence on the possible binary origin of the nucleus of HB 12, we examine closely the spectra taken on September 26, 2005 photospheric absorption features characteristic of a cool companion. The spectrum between 4150 and 4550 Å is shown in Figure 6a in an expanded scale. Apparent G-band feature characteristic of late type stars is seen, and the molecular CN λ4216 absorption can also be identified. Furthermore, absorption features due to the s-process elements such as Y and Sr were found in the spectrum with Y II λ4178 and Sr I λ4607 being the primary features. The molecular $C^{13}C^{13}$ λ4752 is also seen in absorption in the spectrum as shown in Figure 6b. The spectrum ranges from 5150 to 5600 Å clearly indicates C_2 features at λ5165 and λ5585 and is presented in Figure 6c. The Mg I triplet ($\lambda\lambda$5167-72-83) is also marginally seen in the spectrum.

The above mentioned features seems to suggest the existence of a cool companion with a spectral type of G to early K to the exciting source of HB 12. However, this introduces discrepancy with our mass estimation based on the lightcurves, which gives a spectral type of M. Note that a M dwarf in isolation can not be detected at all at the distance of HB 12 of about 2.24 kpc (Cahn et al., 1992). This discrepancy can not be reconciled unless additional physical processes are involved. The spectral change of the cool secondary is here attributed to most likely external heating of its upper atmosphere by the hot primary (Grauer and Bond, 1983). Further investigations of this system based on high resolution spectroscopic

observations is highly needed to have this issued resolved, which may come up with a more reliable determination of the spectral type of the secondary. However, this uncertainty with the spectral determination does not affect in any way our inference of the binary origin of the nucleus of HB 12 based on our photometric results.

6. Summary

Based on the time-series multi-band photometric observations and low-resolution spectroscopy, our study of the physical nature of the nucleus (NSV 26083) of the young PN HB 12 has led to the following results:

1. The central star is probably a close binary with an orbital period of 3.4 hrs. This provides further support to the theory of a binary origin of bipolar PNe.

2. The difference in the R and I lightcurves is indicative of a reflection effect of the illuminated surface of the secondary.

3. Assuming a mass of 0.6 $M_\odot$ of the primary, an upper limit mass and radius of the secondary star can be estimated to be $M_2 < 0.443\ M_\odot$ and $R_2 < 0.403\ R_\odot$, respectively. This results in an estimation of a physical separation of $\sim 1.163\ R_\odot$ of the close binary in association with NSV 26083. The hemisphere of the secondary can be suffering from reflection and heating effects from the hot primary. This thermal coupling may well lead to a spectral change of the secondary and deserve to be investigated further in detail.

Acknowledgments

We are grateful to the Reviewer for useful comments, and Prof. Sun Kwok at University of Hong Kong, Prof. Yi Chou at National Central University, and Dr. Yu-Lei Qiu, Dr. Jian-Yan Wei, and Prof. Jing-Yao Hu at National Astronomical Observatory of the Chinese Academy of Sciences for useful discussions. This work was partially supported by the National Science Council of Taiwan under NSC 93-2752-M-008-001-PAE, NSC 93-2112-M-008-006, NSC 94-2752-M-008-001-PAE, and NSC 94-2112-M-008-002. Finally, we acknowledge funding from the National Natural Science Foundation of China through grant O611081001.

REFERENCES

Arrieta, A. & Torres-Peimbert, S., 2003, ApJS 147, 97

Black, J. H. & van Dishoeck, E. F., 1987, ApJ 322, 412

Bignell, R. C., 1982, Planetary nebulae, Dordrecht : Reidel, 1983, 69

Bruch, A., Vaz, L. P. R. & Diaz, M. P., 2001, A&A 377, 898

Cahn, J., Kaler, J. B. & Stanghellini, L., 1992, A&AS 94, 394

Chen, A., O'Donoghue, D., Stobie, R. S., Kilkenny, D., Roberts, G. & van Wyk, F., 1995, MNRAS 275, 100

Dinerstein, H. L., Lester, D. F., Carr, J. S. & Harvey, P. M., 1988, ApJ 327, L27

De Marco, O., Bond, H. E., Harmer, D., & Fleming, A. J., 2004, ApJ 602, L93

Garcia-Segura, G., Langer, N., R*ó*zyczka, M. & Franco, J. , 1999, ApJ 517, 767G

Garcia-Segura, G., Franco, J. & L*ó*pez, J. A., 2000, ASPC 199, 235G

Grauer, A. D. & Bond, H. E., 1983, ApJ 271, 259G

Hillwig, T., 2004, in Asymmetrical Planetary Nebulae III : Winds, Structure and the Thunderbird, eds. M. Meixner, J. H. Kastner, B. Balick, & N. Soker, ASP Conf. Series, 313, (ASP, San Franciso), 529 (astro-ph/0310043)

Heap, S. R. & Augensen, H. J., 1987, ApJ 313, 268

Hora, J. L. & Latter, W. B., 1996, ApJ 461, 288H

Hora, J. L., Latter, W. B., Dayal, A., Bieging, J., Kelly, D. M., Tielens, A. G. G. M. & Trammell, S. R., 2000, Asymmetrical Planetary Nebulae II : From Origins to Microstructures, ASP Conference Series, Vol. 199.

Kastner, J. H. & Weintraub, D. A., 1994, ApJ 434, 719

Kwok, S., Hrivnak, B. J., Zhang, C. Y. & Langill, P. L., 2000, ApJ 544L, 149K

Miranda, L. F. & Solf, J., 1989, A&A 214, 353M

Morris, M., 1990, fmpn.coll, 520M

Paczy*ń*ski, B., 1981, AcA 31, 1

Rappaport, S., Joss, P. C. & Webbink, R. F., 1982, ApJ 254, 616R

Reid, A. H. N., Bolton , C. T., Crowe, R. A., et al., 1993, ApJ 417, 320

Schönberner, D., 1981, A&A 103, 119

Stasińska, G., Górny, S. K. & Tylenda, R., 1997, A&A 327, 736

Soker, N., 1997, ApJS 112, 487

Soker, N., Rappaport, S. & Harpaz, A., 1998, ApJ 496, 833G

Soker, N., 2000, in "Asymmetrical Planetary Nebulae II : Form Origins to Microstructures", eds. J. H. Kastner, N. Soker & S. Rappaport, ASP Conference Series, Vol. 199, p. 71 (astro-ph/ 9909258)

Sorensen, P. & Pollacco, D., 2004, in Asymmetrical Planetary Nebulae III:Winds,Structure and the Thunderbird, eds. M. Meixner, J. H. Kastner, B. Balick, & N. Soker, ASP Conf. Series, 313, (ASP, San Franciso), 515

Stellingwerf R. F., 1978, ApJ 224, 953

Tylenda, R., Acker, A., Raytchev, B., Stenholm, B. & Gleizes, F., 1991a, A&AS 89, 77T

Tylenda, R., Stasińska, G., Acker, A. & Stenholm, B., 1991b, A&A 246, 221

Weidemann, V., 1989, A&A 213, 155

Welch, C. A., Frank, A., Pipher, J. L., Forrest, W. J. & Woodward, C. E., 1999, ApJ 552, L69

Zhang, C. Y., Kwok, S., 1993, ApJS 88, 137

Zuckerman, B.& Aller, L. H., 1986, ApJ 301, 772

Fig. 1.— The HST/WFPC2 narrow-band [N II] (F658N) image of HB 12, displayed with a linear gray scale. We present here the combined data sets (U6CI0405, U6CI0406, U6CI0407,and U6CI0408) of B. Balick. The total exposure time is 1300 s and the field of view is $18'' \times 18''$. The slit position is shown against the image of the core of the PN.

Fig. 2.— Differential photometric lightcurves of NSV 26083 in both the R band (a) and the I band (b).

Fig. 3.— Power spectra of the time-series photometric data in both R (a) and I (b).

Fig. 4.— Phase diagrams of the photometric data in R (a) and I (b). The periodic variations are believed to be due to an eclipsing binarity nature of the central source. The average error of the phase bin is ± 0.0074 mag for the R band and ± 0.0046 mag for the I band.

Fig. 5.— The spectrum of HB 12 in the wavelength range from 4800 to 7800 Å.

Fig. 6.— Enlarged spectrum of HB12 in the ranges (a) 4150 - 4550 Å, (b) 4550 - 4950 Å, (c) 5150 - 5600 Å.

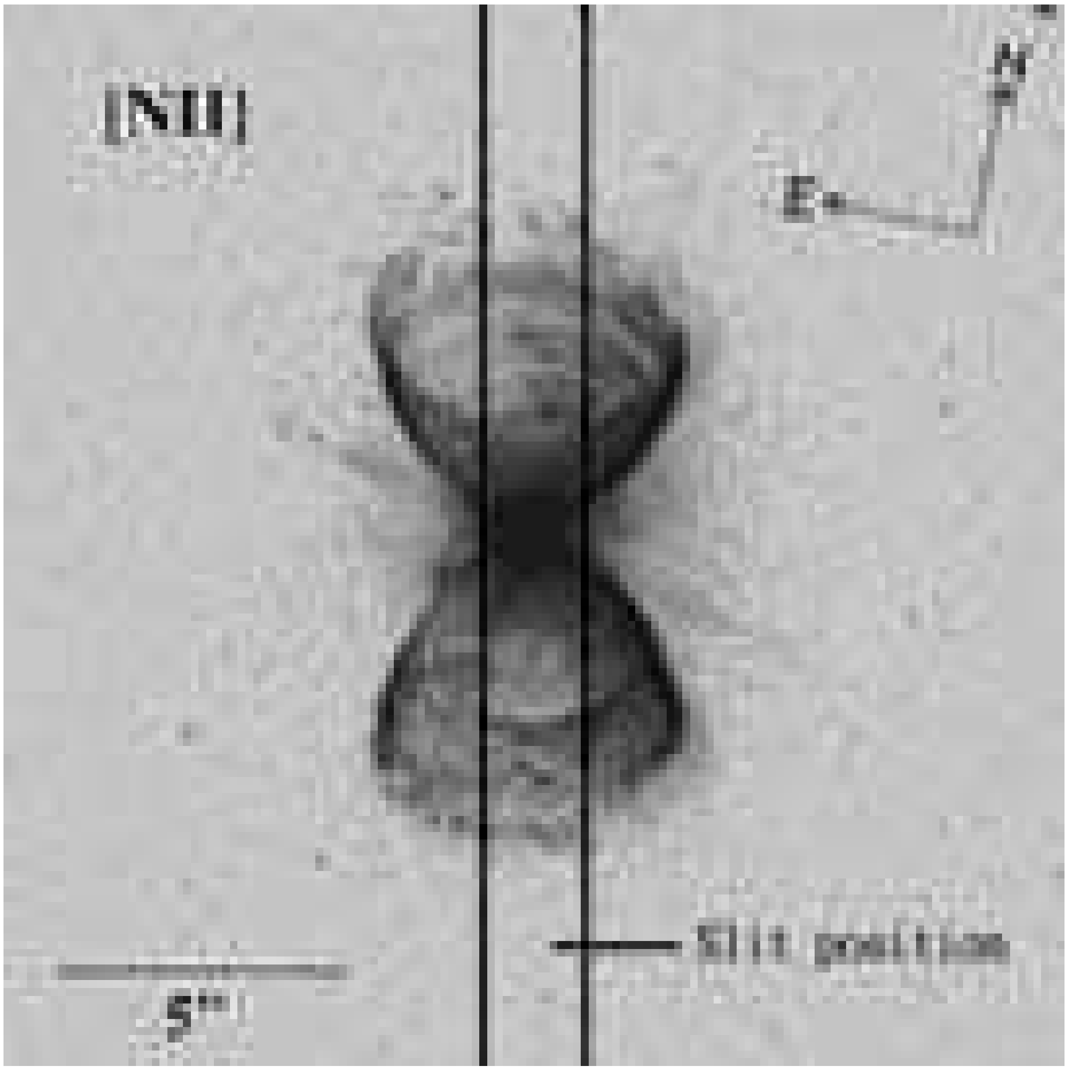

fig.1

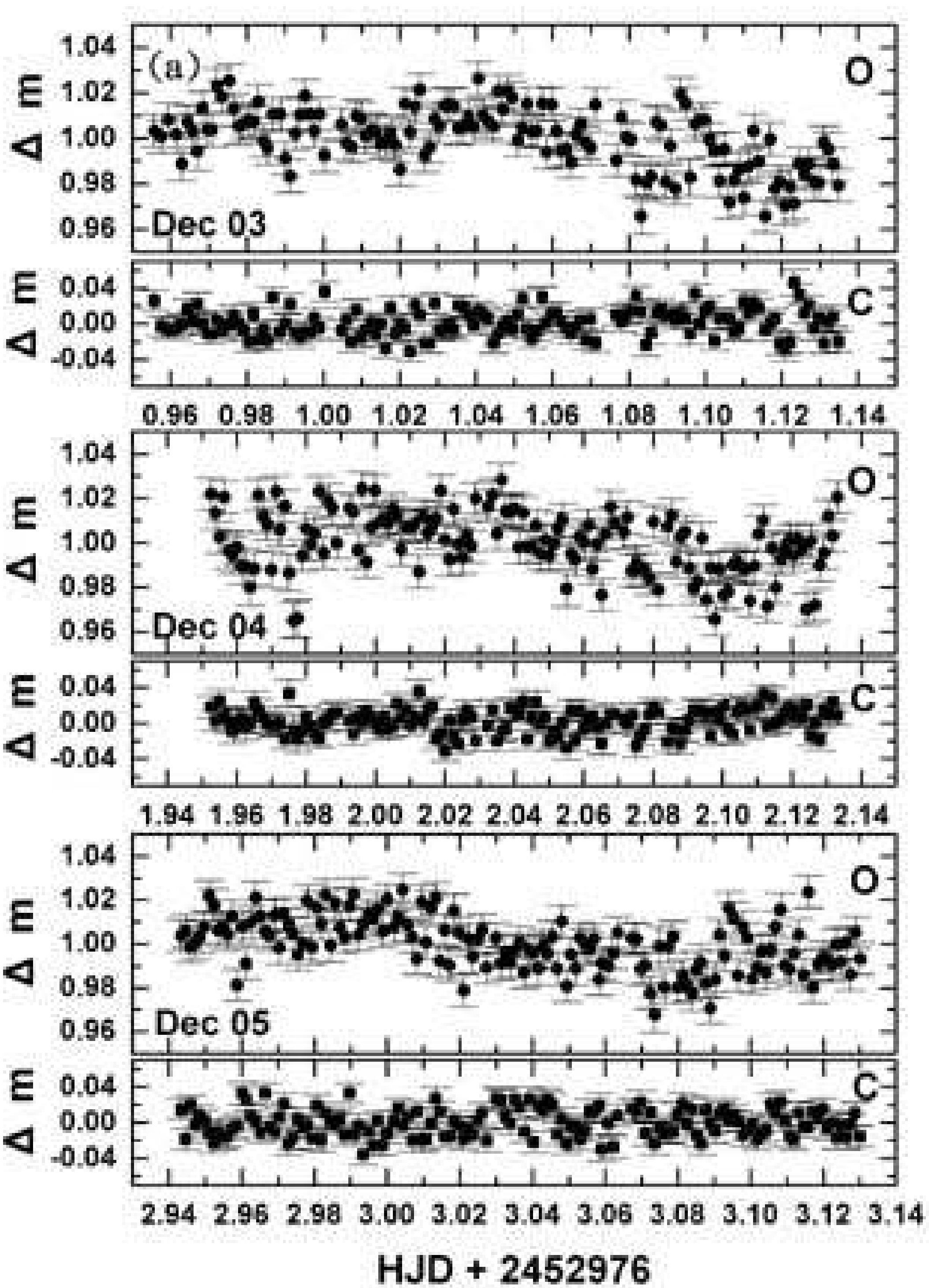

fig.2a

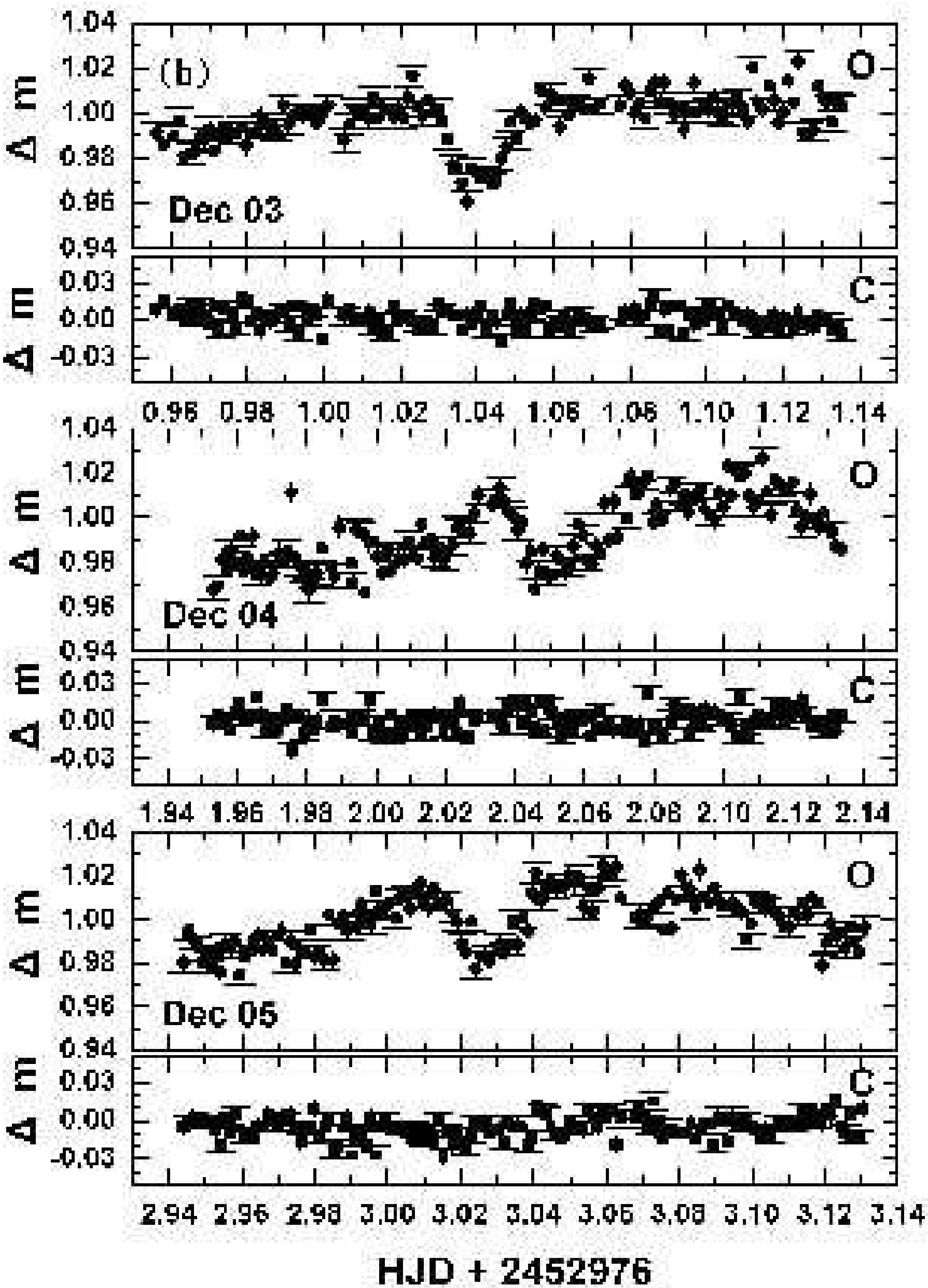

fig.2b

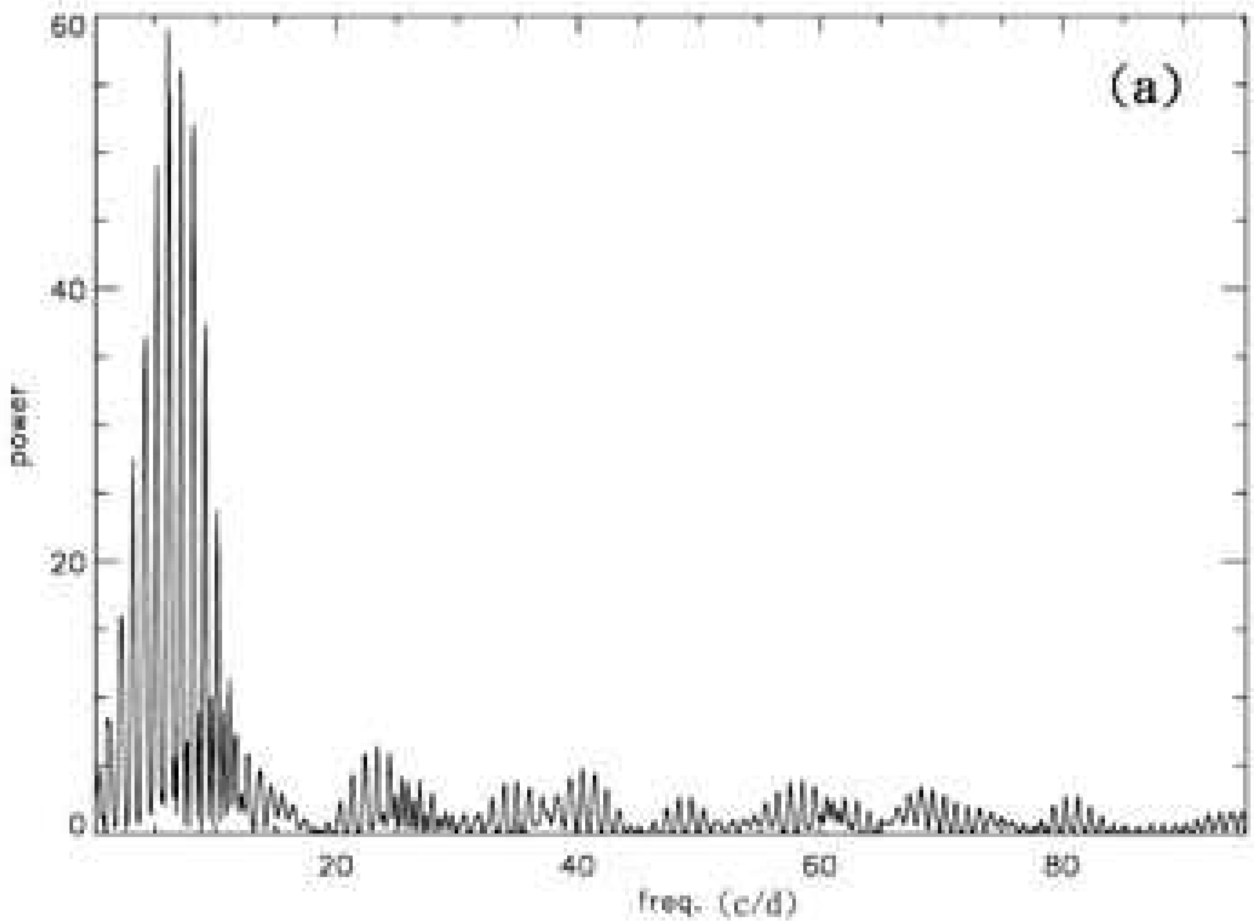

fig.3a

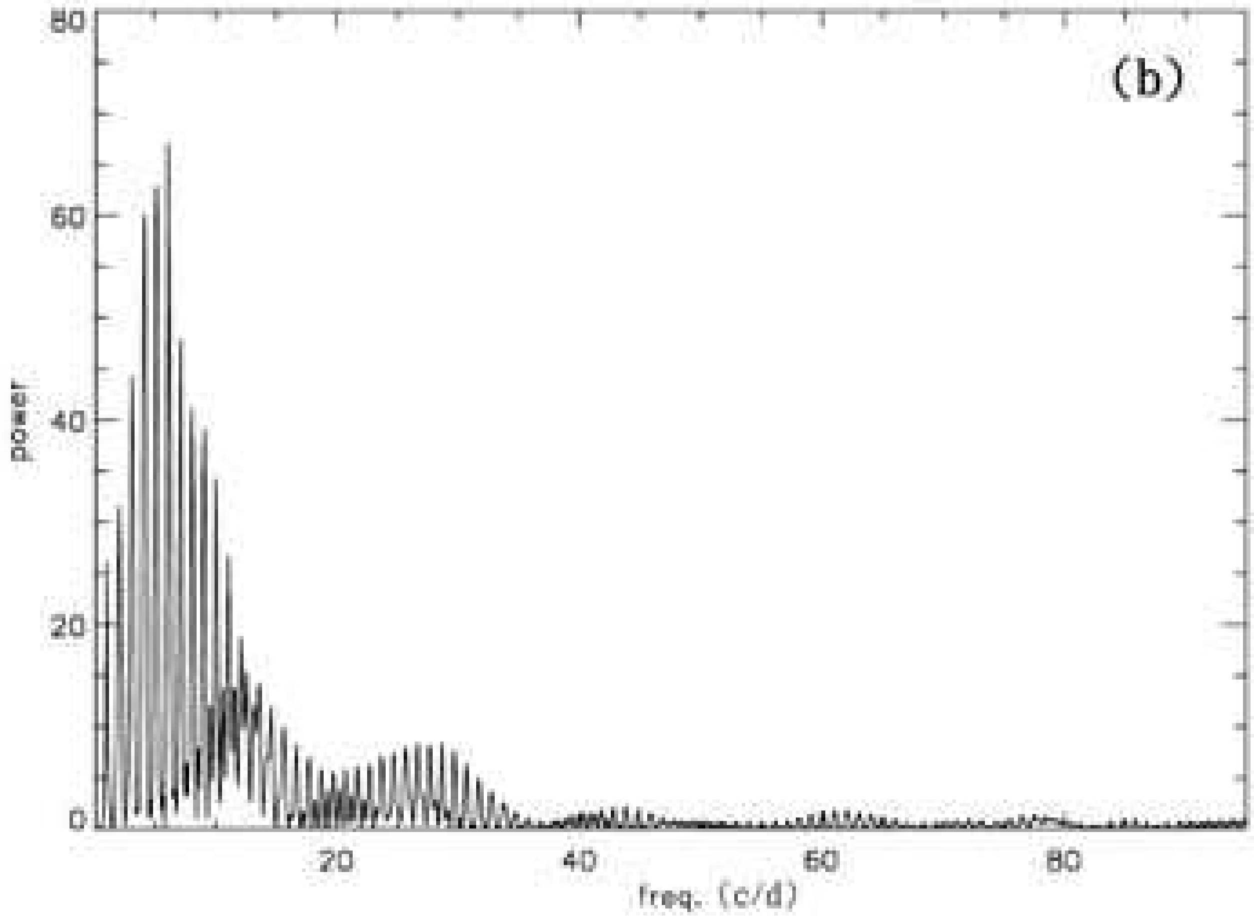

fig.3b

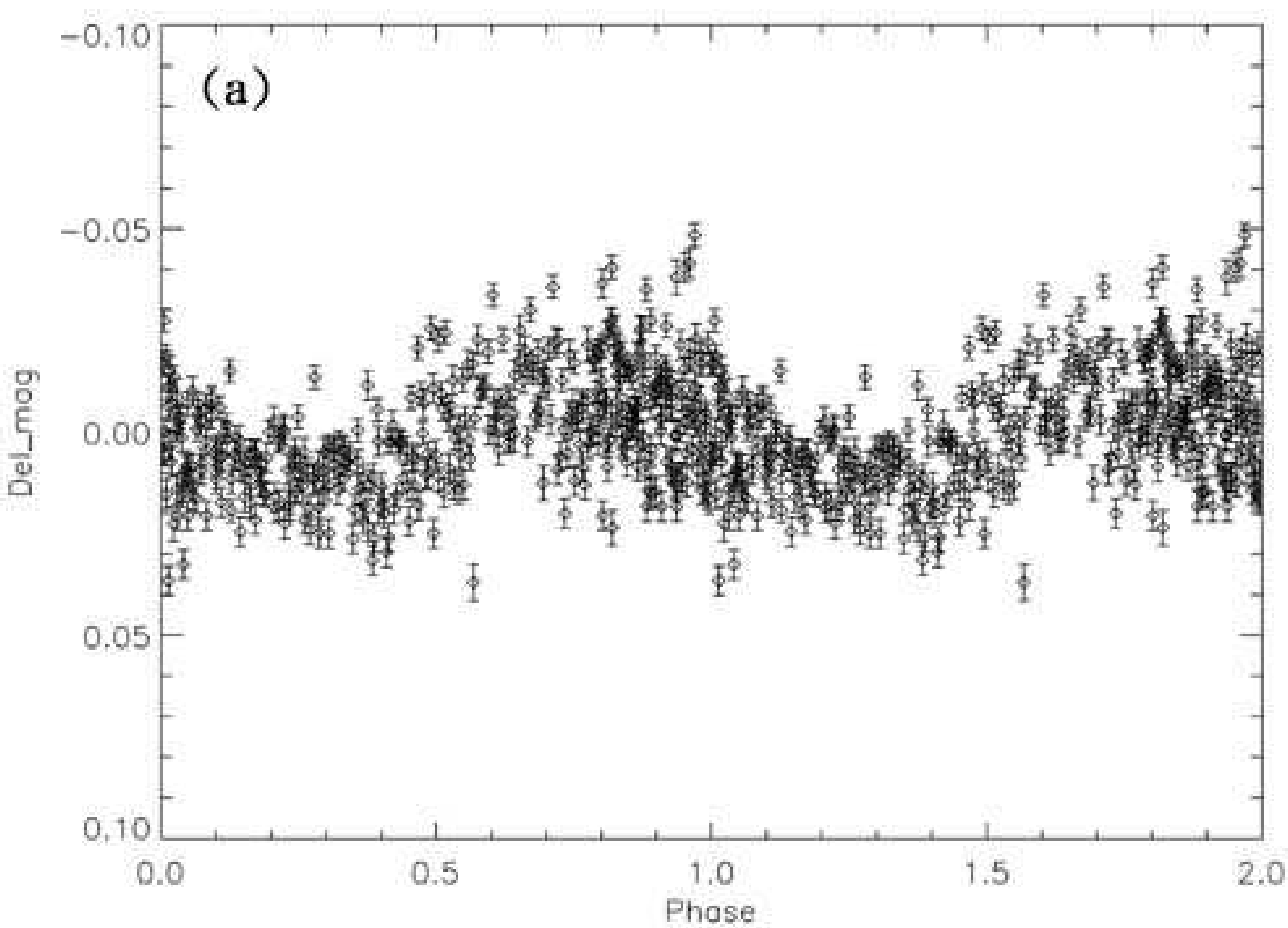

fig.4a

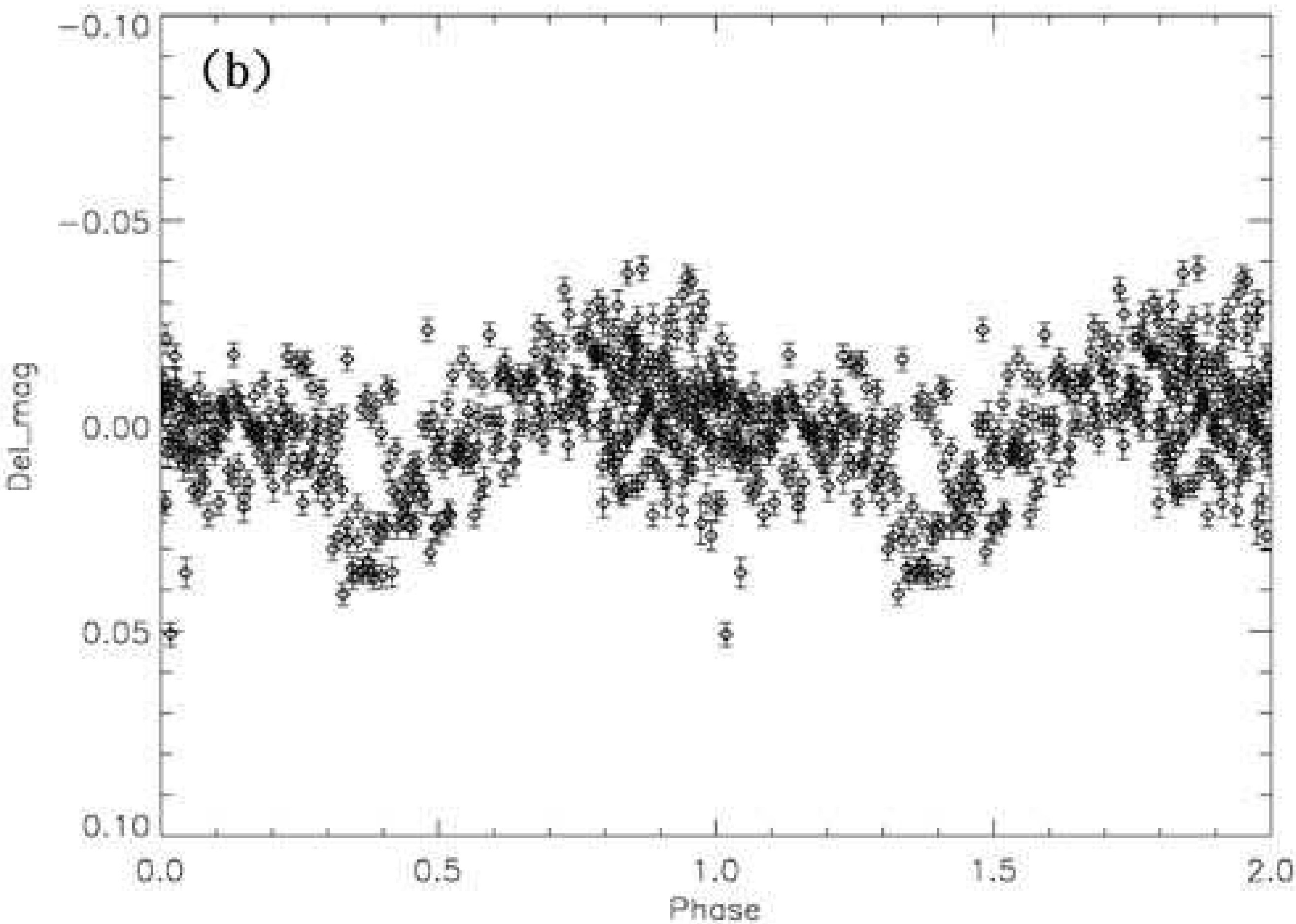

fig.4b

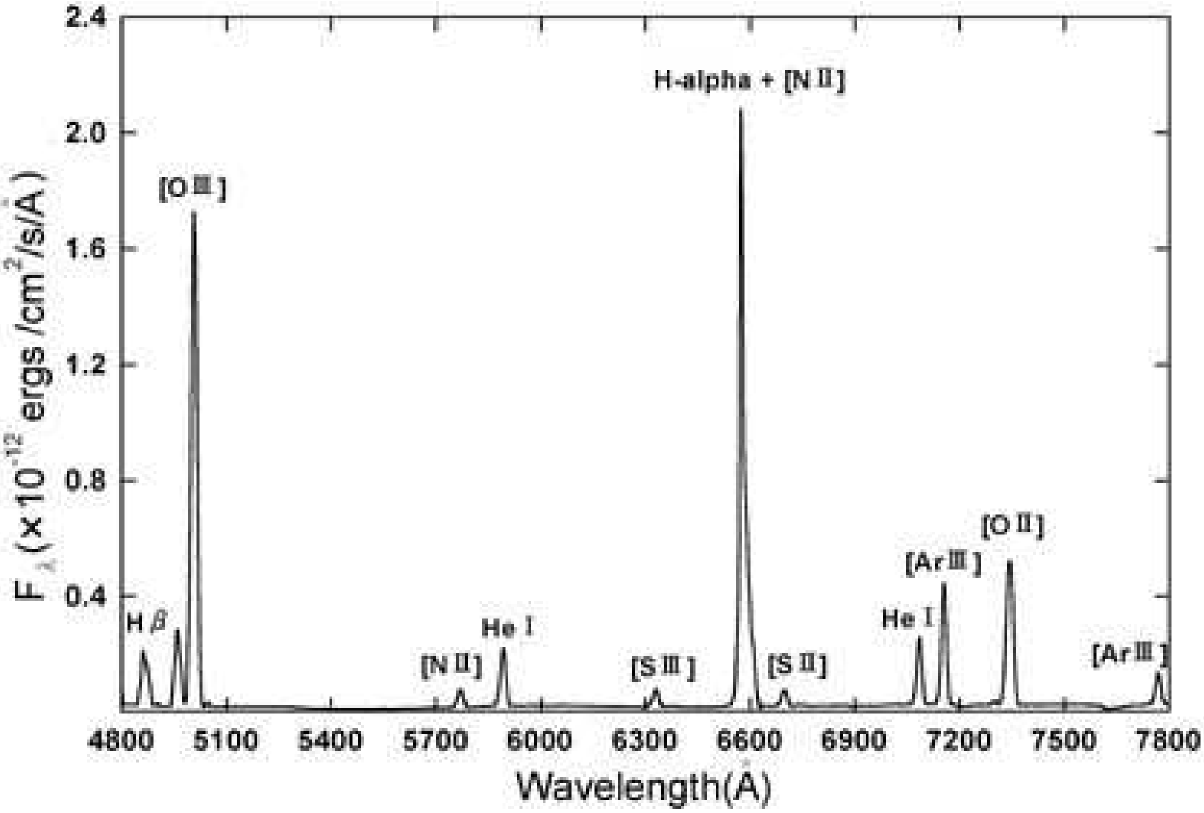
2.4
2.0
1.6
1.2
0.8
0.4
F_λ ($\times 10^{-12}$ ergs /cm^2/s/Å)
H-alpha + [N II]
[O III]
H β
[N II]
He I
[S III]
[S II]
He I
[Ar III]
[O II]
[Ar III]
4800
5100
5400
5700
6000
6300
6600
6900
7200
7500
7800
Wavelength(Å)

fig.5

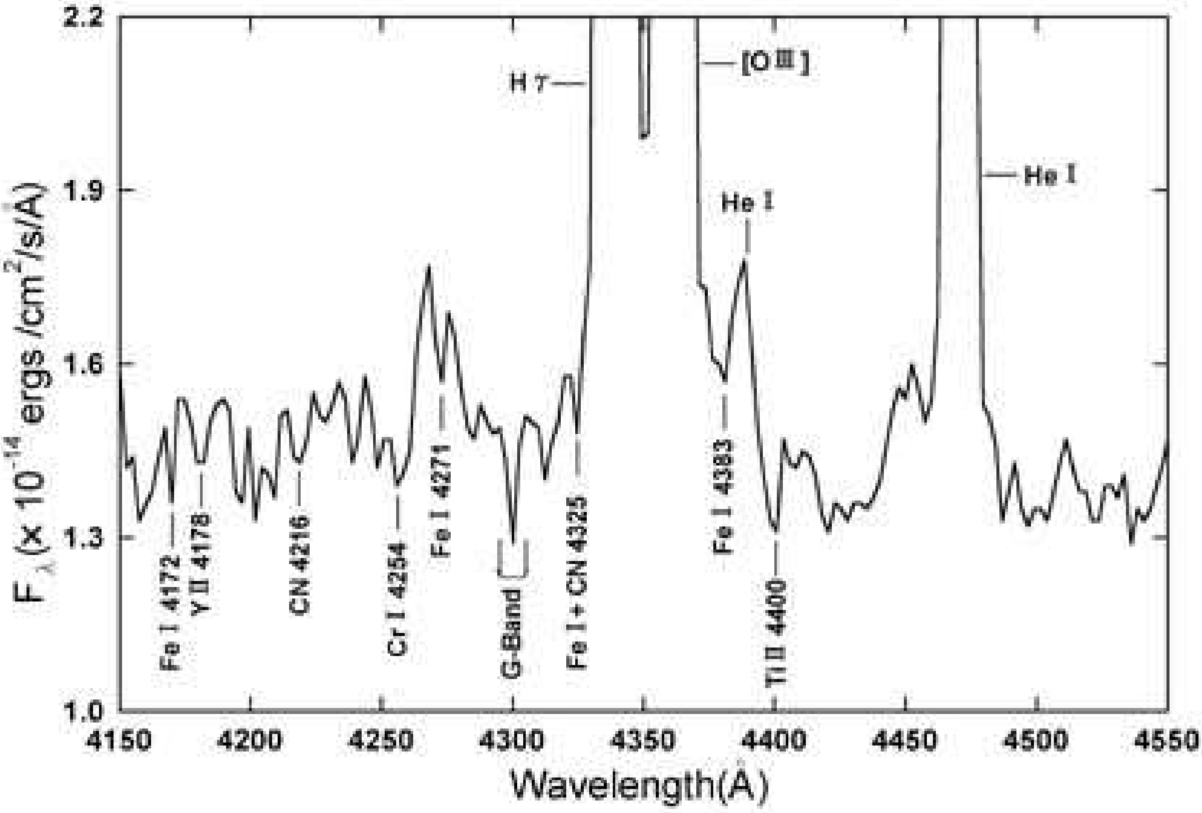
2.2
1.9
1.6
1.3
1.0
4150
4200
4250
4300
4350
4400
4450
4500
4550
Wavelength(Å)
F λ (x 10⁻¹⁴ ergs /cm²/s/Å)
H γ
[O III]
He I
He I
Fe I 4172
Y II 4178
CN 4216
Cr I 4254
Fe I 4271
G-Band
Fe I + CN 4325
Fe I 4383
Ti II 4400

fig.6a

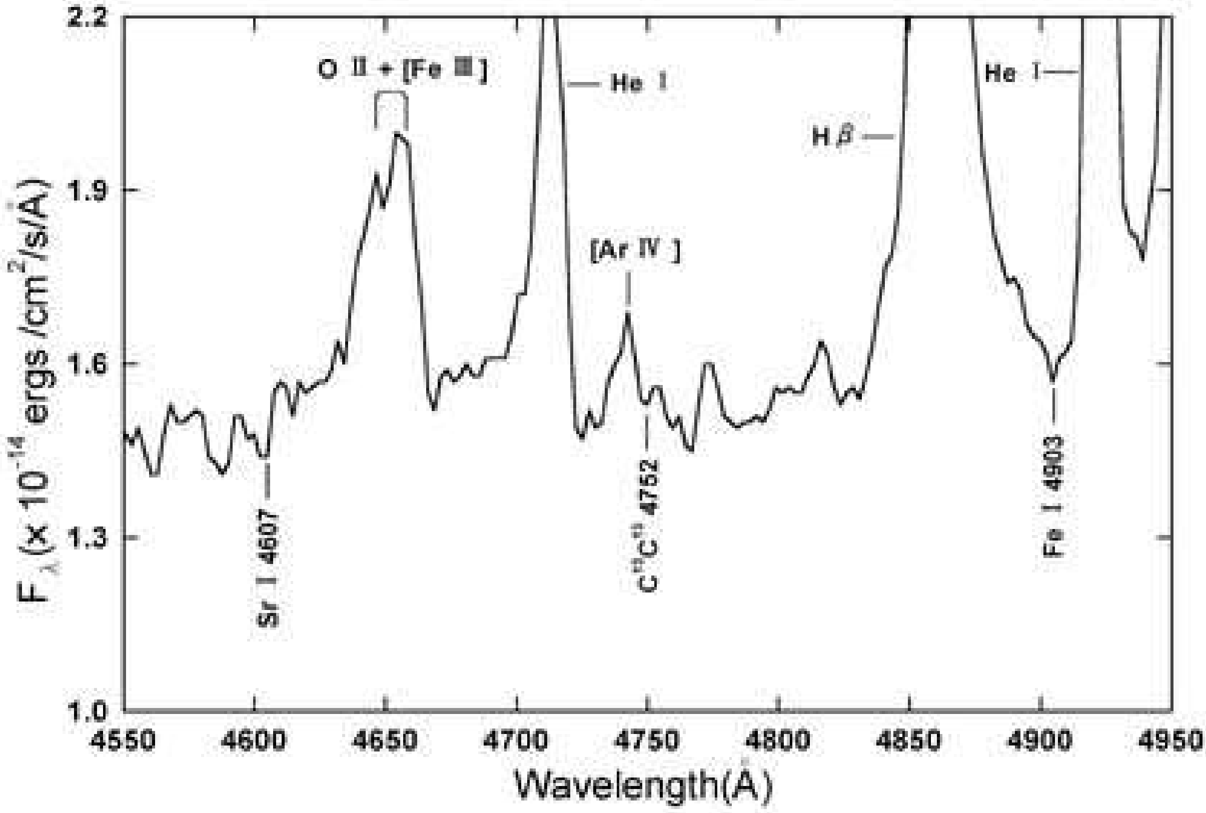
O II + [Fe III]
He I
H β
He I
[Ar IV]
Sr I 4607
C[12]C[13] 4752
Fe I 4903
2.2
1.9
1.6
1.3
1.0
4550
4600
4650
4700
4750
4800
4850
4900
4950
F_λ (x 10^{-14} ergs /cm^2/s/Å)
Wavelength(Å)

fig.6b

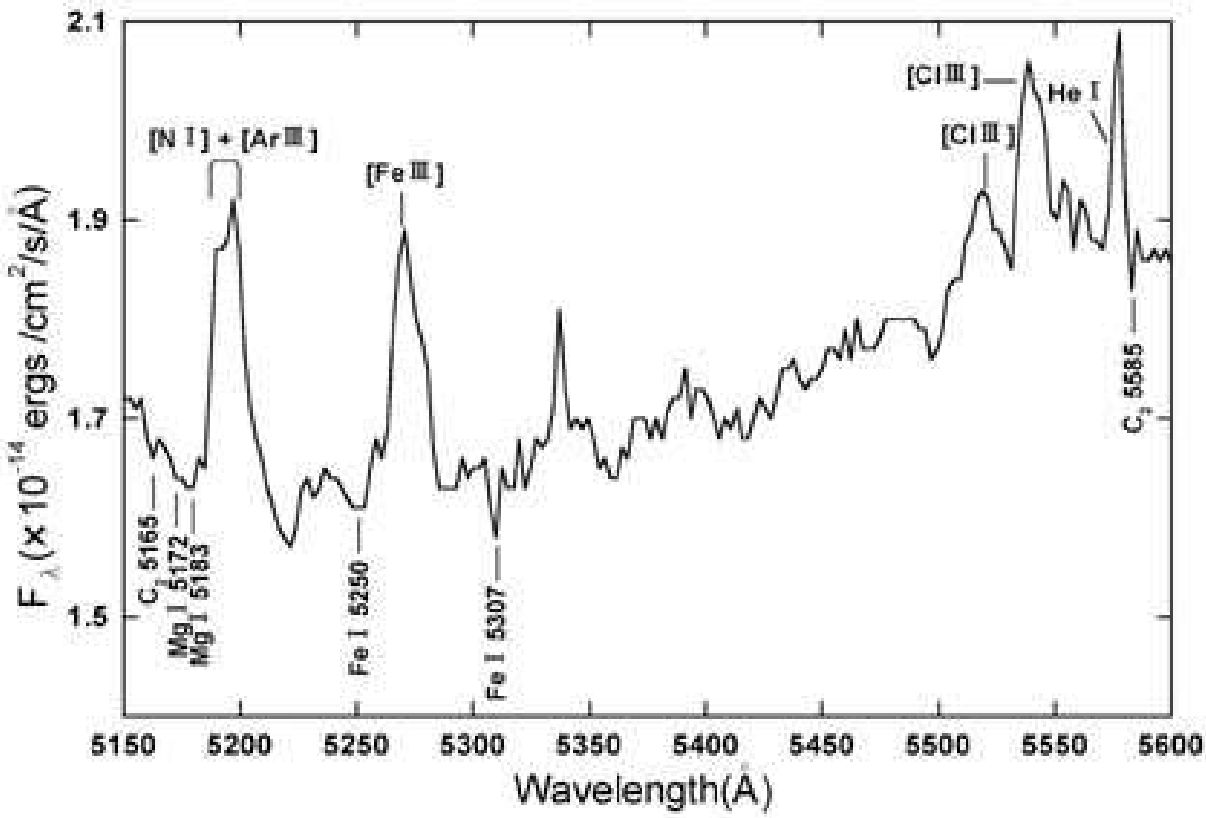
[N I] + [Ar III]
[Fe III]
[Cl III]
[Cl III]
He I
C2 5165
Mg I 5172
Mg I 5183
Fe I 5250
Fe I 5307
C2 5585
2.1
1.9
1.7
1.5
5150
5200
5250
5300
5350
5400
5450
5500
5550
5600
Wavelength(Å)
Fλ (×10⁻¹⁴ ergs /cm²/s/Å)

fig.6c

Table 1. Journal of photometric observations of HB 12

Observation date	Start (UT)	Start (HJD 2452900 +)	Duration (hrs)	Filter	Number of exposures
2003 December 03	10:56	76.9557	4.3	R	132
2003 December 03	10:57	76.9568	4.3	I	132
2003 December 04	10:51	77.9527	4.4	R	139
2003 December 04	10:52	77.9540	4.4	I	139
2003 December 05	10:38	78.9434	4.5	R	143
2003 December 05	10:40	78.9452	4.5	I	143

Table 2. Summary of Journal spectral observations of HB 12

Observation date	Wavelength (Å)	Resolution (Å pixel^{-1})	Width of Slit (arcsec)	Integration Time (s)
2004 Aug 08	4800 - 10500	3.1	3.6	300
2004 Aug 08	4800 - 10500	3.1	3.6	900
2005 Sep 26	3800 - 6200	2.4	2	2 × 3600